

# Demonstration of Atmospheric Lidar Measurement in the Infrared Wavelength Domain with a Superconducting Nanowire Single Photon Detector

Daniela Salvoni<sup>a</sup>, Antonella Boselli<sup>b</sup>, Alessia Sannino<sup>\*c</sup>, Loredana Parlato<sup>c</sup>, Mikkel Ejrnaes<sup>d</sup>, Chengjun Zhang<sup>e</sup>, Lixing You<sup>e</sup>, Xuan Wang<sup>f</sup>, Salvatore Amoruso<sup>c</sup>, Giovanni Piero Pepe<sup>c</sup>

<sup>a</sup>Università degli Studi di Napoli Federico II, Dipartimento di Ingegneria Chimica, dei Materiali e della Produzione Industriale (DICMAPI), Piazzale Vincenzo Tecchio 80, 80125, Napoli

<sup>b</sup>Consiglio Nazionale delle Ricerche (CNR), Istituto di Metodologie per l'Analisi Ambientale (IMAA) C. da S. Loja Z.I. 85050 Tito Scalo (PZ)

<sup>c</sup>Università Degli Studi di Napoli Federico II, Dipartimento di Fisica Ettore Pancini, Via Cinthia, 80126, Napoli

<sup>d</sup>Consiglio Nazionale delle Ricerche (CNR), Superconducting and other Innovative materials and devices institute (SPIN), Via Campi Flegrei 34, 80078, Pozzuoli (NA)

<sup>e</sup>State Key Laboratory of Functional Materials for Informatics, Shanghai Institute of Microsystem and Information Technology (SIMIT), Chinese Academy of Sciences, 865 Changning Rd., Shanghai 200050, China

<sup>f</sup>School of Remote Sensing and Information Engineering Wuhan University, Wuchang District, Wuhan 430072, China  
[alessia.sannino@unina.it](mailto:alessia.sannino@unina.it)

Lidar measurement are widely used today for remote sensing and atmosphere monitoring. Indeed, depending on the specific wavelength adopted, it is possible to determine the presence of specific molecules and pollutants in the atmosphere. Several studies claim that the use of Lidar systems with wavelength larger than 1  $\mu\text{m}$  would provide a special tool for aerosols and carbon dioxide observations. Aerosols measurements are typically performed up to the wavelength  $\lambda = 1064 \text{ nm}$ , while for longer wavelengths they are limited by the detector noise. In this work the results of a preliminary Lidar measurement at  $\lambda = 1064 \text{ nm}$  by using a Superconducting Nanowire Single Photon Detector (SNSPD) are presented. SNSPDs are characterized by high efficiency in the infrared wavelength domain (IR), low noise and dead time, which can in turn enhance the signal quality in Lidar atmospheric measurements at  $\lambda > 1 \mu\text{m}$ , an interesting range for environmental applications. Preliminary measurements have been performed at the University of Naples Federico II by using a NbTiN SNSPD cooled at a temperature of 4.2 K and the Lidar system MALIA. The experimental results at 1064 nm demonstrate the feasibility of the approach for aerosol measurements in the IR, opening the way to further investigations on the use of these detectors for Lidar atmospheric measurements in the IR. The backscattering coefficient,  $\beta$ , has been also estimated and its value is around  $10^{-6} \text{ m}^{-1} \text{ sr}^{-1}$ .

## 1. Introduction

The observation of atmospheric aerosols and pollutants is a relevant scientific and technological topic since these elements play a crucial role in climate changes and badly affect human health (Pöschl, 2005). Due to the importance of this topic, many techniques to sense the particulate locally and remotely have been developed (Lack et al. 2014). In this framework, Light Detection and Ranging (Lidar) technique represents today an extremely precise ground based remote sensing method for acquiring the spatially resolved profile of particulate and molecules content in the atmosphere, up to distances of tens of kilometres. The typical Lidar setup consists of a light emitter (i.e. a high power pulsed laser) pointed toward a target, namely the atmosphere, and a receiver formed by a telescope, a stage of filters for spectral selection, optics elements to redirect the collected beam on a detector and the electronic readout. A sketch of the Lidar setup adopted here

is presented in Figure 1a. As presented in what follows, the analysis of the signal collected by the receiver provides the aerosol content profile as a function of the distance from the emitter, that is the altitude.

Depending on the specific Lidar technique adopted, it is possible to obtain further information about the particulate species and shape (Weitkamp, 2006). Concerning the emitter wavelength, it is chosen according to the species of interest. Indeed, as mentioned by Salvoni et al. (2019), the use of infrared wavelengths can be significant in the study of pollutants and greenhouse gases such as ozone and carbon dioxide. Moreover, the use of IR sources would provide other advantages such as a reduced undesired absorption by the molecular compounds in the air and the reduced risk of injuries, as the lasers in this region are generally eye - safe. The latter would open the way to continuous measurements in urban and industrial areas and would include the Lidar as a validating technique for novel carbon dioxide and particulate absorption methods such as the one presented by Cormos et al. (2019).

The main obstacle in the implementation of IR Lidar systems is represented by the detector efficiency and noise. A solution could be the use of single photon detectors instead of proportional detectors but, even in this case, the detectable wavelength range is limited. Indeed, the efficiency of the most used detectors, such as Si single photon avalanche photodiodes (SPADs) and photomultiplier tubes (PMT), drops down above  $1 \mu\text{m}$ , accompanied also by a significative rise in the noise. It is possible to enlarge the wavelength range up to  $1.7 \mu\text{m}$  with the use of InGaAs SPADS at the cost of an increased detector noise but, above that wavelength, conventional single photon detectors are still missing. In this scenario, SNSPDs represent an optimal candidate in terms of efficiency and noise for IR and far IR applications. Those devices consist of a thin superconducting nanostrip whose thickness and width are about  $5 \text{ nm}$  and  $70 \text{ nm}$ , respectively. The thickness and width can vary slightly according with the superconducting material and the wavelength to be detected (Ejmaes et al. 2017). SNSPD provide almost 100% system detection efficiency in IR and less than 1 cps dark counts rate (Hu et al. 2020). These properties are accompanied by few nanoseconds dead time (Ejmaes et al. 2009), picoseconds temporal resolution and absence of afterpulses. Here a report on the results of a preliminary Lidar measurement with a SNSPD is presented. The operating wavelength is  $1064 \text{ nm}$ , a value typically adopted in Lidar systems for the acquisition of aerosols profiles. The SNSPD is made of NbTiN, a superconducting material which exhibit particularly high performances also at a temperature of  $4.2 \text{ K}$  (liquid helium) and does not require expensive refrigerators. Furthermore, it was demonstrated by Ejmaes et al. (2019) that this temperature regime is suitable for this material to reduce the thermal fluctuations contributing to the noise.

## 2. Device fabrication and measurement setup

The SNSPD used in this measurement is based on a NbTiN thin film ( $5 \text{ nm}$  thick) deposited onto a double-side polished thermally oxidized Si substrates by reactive dc-magnetron sputtering in an Ar + N<sub>2</sub> gas atmosphere, under a total pressure of  $0.27 \text{ Pa}$  at room temperature. A meander shape, i.e. a folded nanostrip, is transferred to the film with electron beam lithography and UV lithography and the final area is a circle with a diameter of  $15 \mu\text{m}$ , the strip width is  $70 \text{ nm}$  and the space among two consecutive strips is  $90 \text{ nm}$ . A SEM image is shown in Figure 1b. Further details on fabrication can be found in Yang X. et al. (2017).

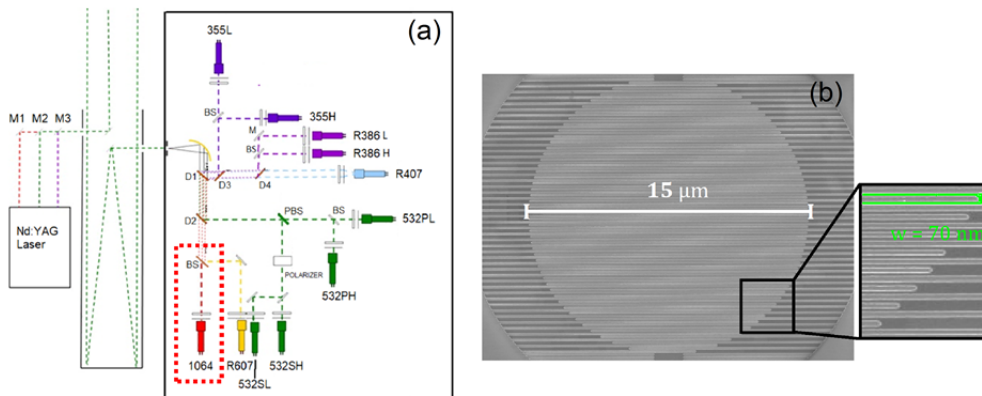


Figure 1: (a) Scheme of MALIA Lidar system. M1, M2, M3 represent the laser wavelengths emitted in the atmosphere ( $1064 \text{ nm}$ ,  $532 \text{ nm}$ ,  $355 \text{ nm}$ ). D1, D2, D3, D4 are the dichroic mirrors used to separate the different wavelengths. BS and PBS are the beamsplitters adopted to divide the signal and the polarizations. The red box highlights the channel used in the present work. (b) A SEM image of NbTiN SNSPD.

The measured critical temperature of the SNSPD is  $T_c = 6.6$  K, hence the measurement could be performed by cooling down the device inside a liquid helium dewar ( $T = 4.2$  K), with the use of a cryogenic insert equipped with a single mode fiber which realizes the optical coupling between the device and the Lidar system.

According with the current assisted detection model described first by Gol'Tsman et al. (2001), an incident photon on the SNSPD generates a hot spot on the nanostrip that is, a resistive region where the local temperature overcomes the critical value  $T_c$ . If a bias current,  $I_b$ , is injected along the nanostrip, due to the presence of the hot spot, it is forced to flow at the edges of the hot spot region where, if  $I_b$  is sufficiently large, a growing resistive belt across the strip is generated (Ejrnaes et al. 2010). The result is a photon-induced voltage pulse (Casaburi et al. 2015) which corresponds to a detection event. The superconducting state is restored as the current is diverted inside an external electrical circuit.

For the device used in this work, the measured critical current is  $I_c = 9.85$   $\mu$ A (Figure 2a) and the measurement was performed at  $I_b = 7.50$   $\mu$ A as, at this bias current value, the dark count rate is low and the counting rate almost reaches its maximum (see Figure 2b). The dark count rate, i.e. the detector intrinsic noise, depends exponentially on the bias current (Nasti et al. 2015) and hence it can be drastically reduced by slightly tuning the bias current even though nontrivial dependence has been observed recently (Salvoni et al. 2020).

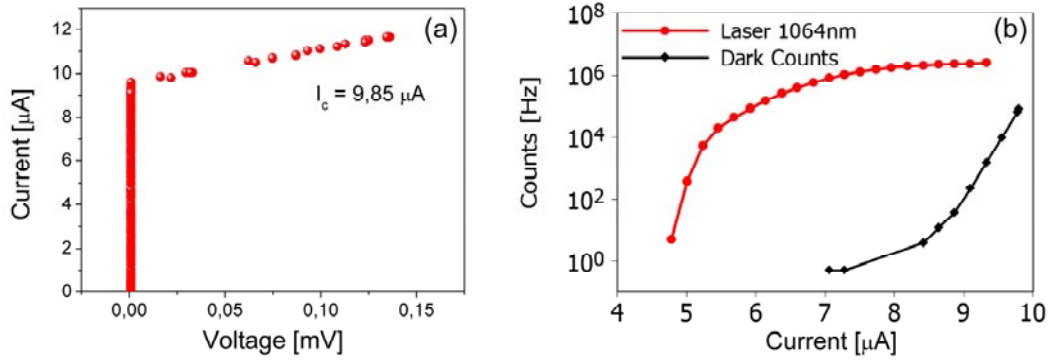


Figure 2: The IV curve is shown in (a). If the current is lower than the critical value, the device remains in the superconducting state ( $\Delta V = 0$ ); when  $I_b > I_c$  the SNSPD enters in a normal state and a resistive IV curve is measured. The dependence of the counting rate at 1064 nm and of the dark count rate (intrinsic noise) on the bias current is shown in (b). The operating current was set to optimise the signal to noise ratio

The Lidar system used in this experiment is the *Multi-wavelength Aerosol Lidar Apparatus* (MALIA), operating at the Physics Department of the University of Naples Federico II (Pisani, 2013). MALIA station, formerly EARLINET (European Aerosol Research Lidar Network) station since 2000, is a National facility of the pan-European Research Infrastructure ACTRIS (Aerosol, Cloud and Trace Gases Research Infrastructure). This system is dedicated to the detection of aerosols masses and water vapor. The setup scheme is presented in Figure 1a, it operates at fundamental (1064 nm), the second (532 nm) and third (355 nm) harmonics, of a pulsed Nd:YAG laser source. The three laser beams are fired in the atmosphere simultaneously. The pulse duration  $\tau$  is 5 ns and the repetition rate is 20 Hz. Maximum pulses energy  $P_0$  is 0.65 J at 1064 nm, 0.15 J at 532 nm and 0.1 J at 355 nm. The laser light undergoes a series of scattering processes due to the presence of atmospheric molecules and particles and the backscattered signal  $P(z, \lambda)$  is collected by a Newtonian telescope with a focal length of 120 cm and a diameter of 30 cm. Different wavelengths and polarizations are then separated by a series of dichroic mirrors and polarizing beam splitters and the signal in each channel is acquired by a detector. The backscattered signal  $P(z, \lambda)$  measured by the detector depends on the setup and on the target species and distance according with the formula presented in Weitkamp (2006):

$$P(z, \lambda) = \frac{P_0 A \frac{\eta c \tau}{2} O(z)}{z^2} \beta(z, \lambda) \exp \left[ -2 \int_0^z \alpha(\lambda, z') dz' \right] \quad (1)$$

where  $z$  represents the target altitude,  $A$  is the telescope area,  $c$  is the light velocity,  $O(z)$  is the overlap function, which accounts for the telescope and beam relative alignment,  $\beta$  is the backscattering coefficient which determines the target species and  $\alpha$  is the extinction coefficient and represents the attenuation due to the atmospheric absorption and scattering.

As one can notice in Eq. (1), the signal power is a function of the distance of a target (single molecule or particle) from the Lidar. Indeed, this technique is based on a measurement of delay between the initial time  $t_0$ , set by the laser trigger, and the time  $t$  when the signal is detected. With the straightforward relation  $\Delta z = c\Delta t/2$  it is possible to calculate the distance of the target by the measurement of temporal delay.

The resolution of Eq. (1) in terms of  $\alpha$  and  $\beta$  coefficients provides range resolved aerosols characterization in terms of concentration and optical properties. A key Lidar parameter is represented by the Lidar Ratio  $LR = \alpha/\beta$ . LR values are well known in literature for different aerosol's types and can be calculated theoretically (Ackermann,1998) as well as being derived directly (Müller et al. 2007). The extinction and backscattering coefficients can be determined separately by means of Raman Lidar techniques (Ansmann et al. 1992).

To couple the 1064 nm signal with the SNSPD single mode fiber, the attenuated signal beam was directed on a telescope formed by two lenses whose focal lengths are 101.6 mm and 25.4 mm. The two lenses are used to reduce the beam size to one fourth to match the acceptance of a collimator (Thorlabs, F810FC-1064) which finally couples the Lidar signal to the SNSPD single mode fiber. The fiber is fixed to the sustain embedding the detector and is equipped with a micro-lens that further focuses the signal on the SNSPD surface.

### 3. Experimental results

The use of superconducting nanowire as highly sensitive detectors for Lidar measurement is becoming a relevant topic for atmospheric observations in the infrared (see Taylor et al. 2019). As mentioned before, a Lidar system operating at  $\lambda > 1\mu\text{m}$  would present many advantages. First, in such a wavelength region, the molecular scattering cross section due to  $\text{N}_2$  molecules in the atmosphere is lower than the one obtained with  $\lambda < 1\mu\text{m}$ ; hence, the aerosol signal is not hidden by the molecular counterpart and becomes clearer. Second, working in the IR would open the way to the detection of other pollutants such as carbon dioxide and ozone. Finally,  $\lambda > 1.5\mu\text{m}$  is an eye-safe regime, allowing the system to operate in urban areas without compromising public safety and health.

The main issue in moving to longer wavelengths is represented by the detectors, which exhibit a dramatic drop in terms of efficiency and increased noise in the IR. For this reason, the use of SNSPD seems to be the simplest solution to increase the performances of aerosols measurements with Lidar technique and to open the way to the observation of other pollutants.

In this section the results of a Lidar measurement with an SNSPD at 1064 nm are presented. The experimental setup is described in the previous section, a NbTiN SNSPD was adopted as this material exhibits lower fluctuations and noise (Parlato et al. 2020) and it can operate also at the temperature of 4.2 K. During this daytime measurement, it was possible to acquire the signal due to a low altitude cloud and to calculate the  $\beta$  coefficient. Even though this is just a preliminary result, it proves that SNSPD can represent good candidates for Lidar measurements in IR.

#### 3.1 Data acquisition and analysis

During the measurement, the NbTiN SNSPD was kept at the fixed temperature of 4.2 K by dipping a cryogenic insert in a liquid helium dewar and it was polarized at  $I_b = 7.50\mu\text{A}$  to optimize the signal to noise ratio (see Figure 2b). The first operation was to align the laser beam, the telescope and the SNSPD to maximize the signal incident on the device. Then, as shown for example in Figure 3, it was verified that the signal can be clearly distinguished from the background noise by comparing signals registered with the laser illuminating the atmosphere and with the laser stopped but with telescope open. The exemplificative signals reported in Figure 3 refer to an acquisition time of two minutes.

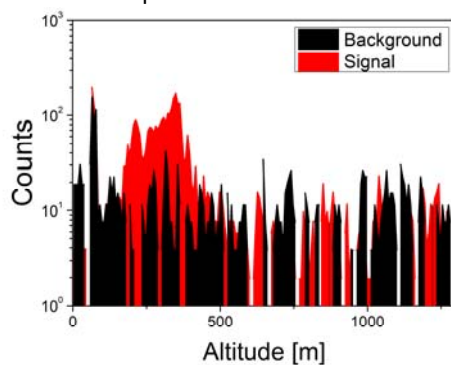


Figure 3: The red (black) area represents the result of a Lidar measurement when the laser is turned on (off). The first peak is due to secondary reflections of the laser beam in the lab.

After this first check, the signal was acquired with two minutes' time integration and a 7 meters' spatial resolution, although low variable clouds were present above the measurement area.

Figure 4 reports the range corrected Lidar signal (Figure 4a) and the aerosol backscattering coefficient profile (Figure 4b) obtained from diurnal observations carried out from 10:06 to 10:08 a.m. in Naples. The estimated value of the backscattering coefficient lays between  $5 \times 10^{-6}$  and  $10 \times 10^{-6} \text{ m}^{-1} \text{ sr}^{-1}$  and it can be compared to the ones obtained in Naples in similar weather conditions at low altitudes.

It is to be noted that the reported Lidar data are not corrected for the overlap function  $O(z, \lambda)$  and they are then underestimated for altitudes below 300 m. Moreover, as Figure 4a reports, Lidar data well fit with the molecular profile at 1064 nm (red line) for altitude above 800 m, where no aerosol layer was present.

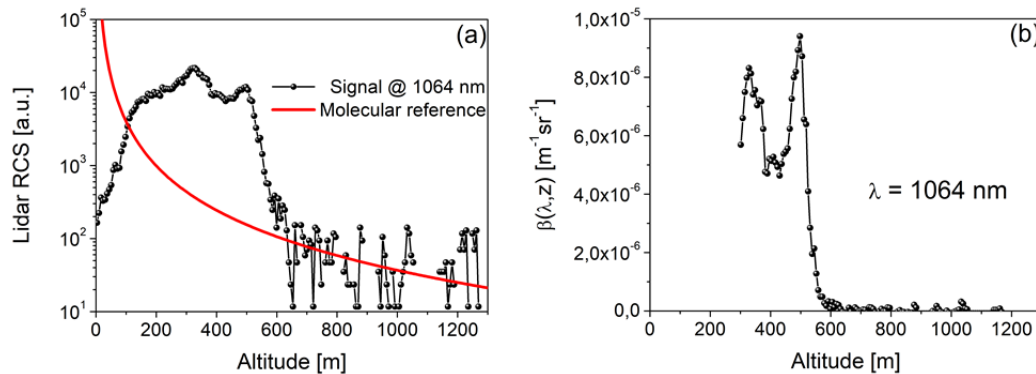


Figure 4: (a) Lidar signals at 1064 nm measured with a SNSPD detector. The black line represents the signal measured within a temporal window of 2 minutes. The red line represents the contribution due to the molecular atmospheric components, calculated analytically at  $\lambda = 1064 \text{ nm}$ . (b) Backscattering coefficient estimated from the measurement in Figure 4a. The initial altitude is shifted as the overlap function  $O(z, \lambda)$  approaches the unity for  $z > 300 \text{ m}$  at  $\lambda = 1064 \text{ nm}$ .

Diurnal data retrieval was obtained following the Klett - Fernald inversion procedure (Klett, 1981; Fernald, 1984) and assuming a LR of 20sr in the cloud range (500 - 600 m) and a LR of 50 sr along the vertical profile, as typically measured in the Naples area at lower altitudes.

The obtained results, even though preliminary and acquired during no clear sky conditions, are promising and demonstrate the feasibility of the use of this new detector for Lidar measurement in the IR domain.

#### 4. Conclusions

In this work it was demonstrated that it is possible to integrate a Superconducting Nanostrips Single Photon Detectors in a Lidar setup. Indeed, the results of a preliminary aerosol measurement at 1064 nm with a combined setup are presented.

It was possible to acquire a clear signal at 1064 nm during two minutes of acquisition, which can be considered a relatively short time. Despite this fact, the dataset was accurate enough to calculate the backscattering coefficient below 1500 m, estimated around  $5 \times 10^{-6}$  and  $10 \times 10^{-6} \text{ m}^{-1} \text{ sr}^{-1}$ . This value can be compared to the beta coefficients calculated in Naples at low altitudes in similar weather conditions. This result sets an optimal starting point for further and more accurate atmospheric Lidar measurements with SNSPD, such as a comparison with the aerosol signal acquired with conventional detectors and with different wavelengths.

#### Acknowledgments

This work was carried out in the context of OT4CLIMA project, funded by the Italian Ministry of Education, University and Research, within the PON 2014-2020 Industrial Research program.

The activities have received funding from the European Union Horizon 2020 research and innovation programme under grant agreement No 654109, ACTRIS2 project.

The research presented here was partially supported by ALA S.r.l., *Advanced Lidar Applications*.

## References

- Ackermann J., 1998, The extinction-to-backscatter ratio of tropospheric aerosol: A numerical study, *Journal of atmospheric and oceanic technology*, 15(4), 1043-1050.
- 15, 746–748, doi:10.1364/OL.15.000746.
- Ansmann A., Wandinger U., Riebesell M., Weitkamp C., & Michaelis W., 1992, Independent measurement of extinction and backscatter profiles in cirrus clouds by using a combined Raman elastic-backscatter lidar, *Applied optics*, 31(33), 7113-7131.
- Casaburi A., Heath R. M., Ejrnaes M., Nappi C., Cristiano R., & Hadfield R. H., 2015, Experimental evidence of photoinduced vortex crossing in current carrying superconducting strips, *Physical Review B*, 92(21), 214512.
- Cormos A. M., Dragan S., Petrescu L., Chisalita D. A., Szima S., Sandu V. C., & Cormos, C. C., 2019, Reducing Carbon Footprint of Energy-Intensive Applications by CO<sub>2</sub> Capture Technologies: An Integrated Technical and Environmental Assessment, *Chemical Engineering Transactions*, 76, 1033-1038.
- Ejrnaes M., Salvoni D., Parlato L., Massarotti D., Caruso R., Tafuri F., Yang X. Y., You L. X., Wang Z., Pepe G. P. & Cristiano, R., 2019, Superconductor to resistive state switching by multiple fluctuation events in NbTiN nanostrips. *Scientific reports*, 9(1), 1-6.
- Ejrnaes M., Parlato L., Arpaia R., Bauch T., Lombardi F., Cristiano R., Tafuri F. & Pepe, G. P., 2017, Observation of dark pulses in 10 nm thick YBCO nanostrips presenting hysteretic current voltage characteristics, *Superconductor Science and Technology*, 30(12), 12LT02.
- Ejrnaes M., Casaburi A., Mattioli F., Leoni R., Pagano S., & Cristiano R., 2010, Time-resolved observation of fast hotspot dynamics in superconducting nanowires, *Physical Review B*, 81(13), 132503.
- Ejrnaes M., Casaburi A., Cristiano R., Quaranta O., Marchetti S., & Pagano S., 2009, Maximum count rate of large area superconducting single photon detectors, *Journal of Modern Optics*, 56(2-3), 390-394.
- Fernald F. G., 1984, Analysis of atmospheric lidar observations: some comments, *Applied optics*, 23(5), 652-653.
- Gol'Tsman G. N., Okunev O., Chulkova G., Lipatov A., Semenov A., Smimov K., Voronov B., Dzardanov A., Williams C. & Sobolewski, R., 2001, Picosecond superconducting single-photon optical detector, *Applied physics letters*, 79(6), 705-707.
- Klett J. D., 1981, Stable analytical inversion solution for processing lidar returns, *Applied optics*, 20(2), 211-220.
- Hu P., Li H., You L., Wang H., Xiao Y., Huang J., Yang X., Zang W., Zhen W. & Xie, X., 2020, Detecting single infrared photons toward optimal system detection efficiency, *Optics Express*, 28(24), 36884-36891.
- Lack D. A., Moosmüller H., McMeeking G. R., Chakrabarty R. K., & Baumgardner D., 2014, Characterizing elemental, equivalent black, and refractory black carbon aerosol particles: a review of techniques, their limitations and uncertainties, *Analytical and bioanalytical chemistry*, 406(1), 99-122.
- Müller D., Ansmann A., Mattis I., Tesche M., Wandinger U., Althausen D. & Pisani, G., 2007, Aerosol-type-dependent lidar ratios observed with Raman lidar, *Journal of Geophysical Research: Atmospheres*, 112(D16).
- Nasti U., Parlato L., Ejrnaes M., Cristiano R., Taino T., Myoren H., Sobolewski R. & Pepe G. P., 2015, Thermal fluctuations in superconductor/ferromagnet nanostripes, *Physical Review B*, 92(1), 014501.
- Parlato L., Salvoni D., Ejrnaes M., Massarotti D., Caruso R., Satariano R., Tafuri F., Yang X. Y., You L., Wang Z. & Pepe, G. P., 2020, The Role of Multiple Fluctuation Events in NbN and NbTiN Superconducting Nanostrip Single-Photon Detectors. *Journal of Low Temperature Physics*, 1-6.
- Pisani G., Lidar study of high-density aerosol clouds: The Aerosol Multi-wavelength Polarization lidar Experiment, 2013, PhD thesis, University of Naples Federico II, Naples (Italy).
- Pöschl U., 2005, Atmospheric aerosols: composition, transformation, climate and health effects, *Angewandte Chemie International Edition*, 44(46), 7520-7540.
- Salvoni D., Ejrnaes M., Parlato L., Yang X. Y., You L. X., Wang Z., Pepe G. P. & Cristiano, R., 2020, Dark counts double switching rates in NbTiN Superconducting Nanowire Single Photon Detectors, In *Journal of Physics: Conference Series* (Vol. 1559, No. 1, p. 012016), IOP Publishing.
- Salvoni D., Ejrnaes M., Parlato L., Sannino A., Boselli A., Pepe G. P., Cristiano R. & Wang, X., 2019, Lidar techniques for a SNSPD-based measurement, *Journal of Physics: Conference Series*, v. 1182, n. 1, p. 012014.
- Taylor G. G., Morozov D., Gemmell N. R., Erotokritou K., Miki S., Terai H., & Hadfield R. H., 2019, Photon counting LIDAR at 2.3  $\mu\text{m}$  wavelength with superconducting nanowires, *Optics Express*, 27(26), 38147-38158.
- Weitkamp C., *Lidar: range-resolved optical remote sensing of the atmosphere*, 2006, Springer Science & Business, Vol. 102
- Yang X., You L., Zhang L., Lv C., Li H., Liu X., Zhou H. & Wang, Z., 2017, Comparison of superconducting nanowire single-photon detectors made of NbTiN and NbN thin films, *IEEE Transactions on Applied Superconductivity*, 28(1), 1-6.